Biases in modeled surface snow BC mixing ratios in prescribed-aerosol climate model runs

S. J. Doherty*
Joint Institute for the Study of the Atmosphere and Ocean
University of Washington
3737 Brooklyn Ave NE
Seattle, WA 98195

C. M. Bitz
Department of Atmospheric Sciences
408 ATG, Box 351640
University of Washington
Seattle, WA 98195

M. G. Flanner
Dept. of Atmospheric, Oceanic and Space Sciences
University of Michigan
2455 Hayward St.
Ann Arbor, MI 48109-2143

** Corresponding author*: sarahd@atmos.washington.edu

Introduction

Model studies indicate that black carbon (BC) deposited on snow and sea ice produces climatically significant radiative forcing at both global and regional scales by reducing surface albedo ("BC albedo forcing") (e.g. Warren and Wiscombe, 1980; Hansen and Nazarenko, 2004; Jacobson et al., 2004; Flanner et al., 2007). Global, annual average radiative forcing by BC in snow has been assessed as +0.04 W/m^2 using model estimates adjusted to observed snow concentrations (Bond et al., 2013; Boucher et al., 2013). BC snow albedo forcing has been cited in particular as a possible contributor to warming in the Arctic (e.g. Flanner et al., 2007; Koch et al., 2009), reduced springtime Eurasian snow cover (Flanner et al., 2009), melting of glaciers on the Tibetan Plateau and Himalayan mountains (Xu et al., 2009; Kopacz et al., 2011), and changes in the Asian hydrological cycle (Qian et al., 2011). Estimates of this BC albedo forcing and the resulting climate impacts rely on modeling and therefore on accurate model representation of surface snow BC concentrations.

A critical difference between forcing by BC in the atmosphere and BC in snow is that forcing by BC in the atmosphere scales with the vertically-resolved *burden* of BC (e.g. kg per m^2 of air column), while forcing by BC in snow scales with the *mixing ratio* of BC (e.g. kg BC per kg of snow) in the surface snow layer. This difference is because snow is a highly scattering medium so incident sunlight only penetrates to ~10cm depth, depending on the snow density, grain size and the mixing ratio of absorbing impurities. Therefore BC deeper in the snowpack doesn't produce significant forcing. Surface snow BC mixing ratios are determined by the mixing ratio of BC in snowfall (wet deposition), the settling of atmospheric BC onto the snow surface (dry deposition) and in-snow processes that reduce the amount of snow (melting, sublimation) or that reduce the amount of BC (wash-out of BC with snow meltwater). It is perhaps unsurprising that sublimation is effective at raising surface snow BC mixing ratios. Empirical evidence has shown that when snow melts, the melt water washes down through the snowpack more efficiently than do particulate impurities, also leading to enhanced BC concentrations at the snow surface (Conway et al, 1996; Xu et al., 2012; Doherty et al. 2013; Forsström et al.,

2013). For models to accurately represent snow BC mixing ratios, they must simulate all of these processes with fidelity.

To date, the Community Earth System Model version 1 (CESM1) is the only global climate model that accounts for all of these processes, through the SNow, ICe, and Aerosol Radiative model (SNICAR, Flanner et al., 2007) in the land component (known as the Community Land Model version 4, CLM4; Lawrence et al, 2012), which accounts for snow on land among other things. A more simplified treatment of BC in snow that is on sea ice and in the sea ice itself is also included in the most recent version of the CESM sea ice model component, CICE4 (Holland et al, 2012). In addition to treating processes that determine snow BC mixing ratios, SNICAR captures both fast and slow feedbacks that amplify the radiative forcing by BC in snow: Surface snow warmed by BC absorption generally transforms to larger snow grain sizes, which further reduces snow albedo. In addition, the reduction in albedo for a given mixing ratio of BC is greater for larger-grained snow (Fig. 3 of Flanner et al., 2007). These feedbacks further accelerate warming and lead to earlier snow melt, which in turn leads to higher BC mixing ratios in surface snow as described above. Eventually this also leads to earlier exposure of the underlying surface, further reducing surface albedo (i.e. the classic "snow albedo feedback") (Flanner et al., 2007; Flanner et al., 2009; Figure 29 of Bond et al., 2013).

This comprehensive treatment in CESM1 made possible the recent Atmospheric Chemistry and Climate Model Intercomparison Project (ACCMIP) studies where BC albedo forcing was estimated for surface deposition fields derived from a suite of climate models (Lee et al., 2013). This forcing was included in an overall assessment of modeled radiative forcing under ACCMIP (Shindell et al., 2013). In the Lee et al. study, each participating ACCMIP model calculated BC atmospheric abundances and deposition rates using a common set of emissions. The resulting deposition fields (e.g. grams BC deposited per m^2 per sec in each gridbox/day) were then used in CESM1 to calculate snowpack BC mixing ratios. Estimated BC albedo forcing for the different models' aerosol fields covered a wide range, reflective of differences in BC transport and deposition rates. Comparisons of the modeled snow BC mixing ratios with observed mixing ratios across the Arctic

and Canadian sub-Arctic showed significant positive model biases for Greenland (a factor of 4-8), a factor of 2-5 low biases over the Arctic Ocean, and agreement to within a factor of 2-3 elsewhere, though with the exception of one model (CESM1-CAM5, which has version 5 of the Community Atmosphere Model) BC mixing ratio biases in the remaining regions were more often positive than negative (see Lee et al., 2013 Table 6).

Goldenson et al. (2012) also used CESM1 with prescribed atmospheric aerosol concentrations and deposition fluxes to compute the climate impacts of BC in snow on both land and sea ice and BC in sea ice. They found significant impacts on surface warming and snowmelt timing due to changes in BC deposition in year 2000 versus year 1850. They also found that forcing by BC in snow on land surrounding the Arctic had a larger impact on Arctic surface temperatures and sea ice loss than did BC deposited on sea ice within the Arctic. On sea ice, Goldenson et al. found poor spatial correlation between modeled and observationally-estimated BC concentrations (see their Figure 3), though the range of concentration is similar; on land, the two are better correlated but the model concentrations tend to be higher, by roughly a factor of two (Goldenson et al., 2012 Figure 4).

Jiao et al (2014) applied CESM to simulate BC in snow on land and sea-ice using deposition fields from the Aerosol Comparisons between Observations and Models (AeroCom) suite of global simulations. In comparison with measurements of BC in Arctic snow and sea-ice (Doherty et al, 2011), they found that models generally simulate too little BC in northern Russia and Norway, while simulating too much BC in snow elsewhere in the Arctic. As with Goldenson et al (2012), they found poor spatial correlation between modeled and measured BC-in-snow concentrations, though the multi-model means, sub-sampled over the measurement domain, were within 25% of the observational mean.

Here we test whether the use of prescribed BC mass deposition rates in CESM, as was done in the Goldenson et al. (2012), Holland et al (2012), Lawrence et al (2012), Lee et al. (2013) and Jiao et al. (2014) studies, produces a bias in surface snow BC mixing ratios, and therefore a bias in snow albedo. The bias being investigated would result from the fact that BC deposition fluxes in CESM

prescribed-aerosol runs are decoupled from snow deposition rates, combined with the fact that the model top snow layer has a fixed maximum thickness and is divided when it exceeds this thickness. Note that the bias being tested for here is independent of any biases due to errors in input emissions or in modeled transport and scavenging rates; it is purely a result of the mathematical approach taken in the model to estimating surface snow BC mixing ratios.

Model runs and offline calculations

Prescribed aerosol fields are derived from prognostic aerosol model runs, where the resulting atmospheric concentrations and dry and wet mass deposition fluxes are saved as model output. This is used as input to the prescribed runs. In prognostic model runs, aerosols are emitted directly or formed from aerosol precursors in the atmosphere. Aerosols and their precursors are transported, dry-deposited to the surface, and scavenged in rain and snowfall according to the modeled meteorology. In prognostic aerosol models, wet deposition of BC occurs only when there is rain or snowfall. The mass of BC wet deposited depends on the amount of precipitation, the ambient BC concentration, and the hygroscopicity of the BC, with these dependencies varying from model to model.

When prescribed, atmospheric aerosol concentrations and deposition fluxes are typically independent of the meteorological fields in the model, as is the case in CESM1; the meteorological fields themselves in these runs may be either prescribed or prognostic. Further, the input aerosol fields are often interpolated in time from monthly means. Therefore the episodic nature of aerosol deposition in reality (owing to wet deposition) is generally absent in prescribed aerosol fields. This was the case for the prescribed aerosol studies of Goldenson et al (2012), Lawrence et al (2012), and Holland et al (2012) and for all integrations of CCSM4 (i.e., CESM1-CAM4) that were submitted to CMIP5 and used in the Lee et al. (2013) and Jiao et al. (2014) studies. In the Lee et al., (2013) and Jiao et al. (2014) studies, these BC deposition fields were then coupled with prescribed meteorology from the Climatic Research Unit (CRU) / National Center for Environmental Prediction (NCEP) reanalysis data for 1996-2000 (Lee et al., 2013) or 2004-2009 (Jiao et al., 2014) to

151 calculate surface snow mixing ratios of BC. The CRU/NCEP data set is described at
152 ftp://nacp.ornl.gov/synthesis/2009/frescati/model_driver/cru_ncep/analysis/read
153 me.htm.
154 To test the effect of using decoupled BC mass and snow mass deposition
155 rates on surface snow BC mixing ratios, we first compare ensembles of prescribed-
156 aerosol and prognostic-aerosol runs of CESM/CAM. The prescribed-aerosol runs
157 use the same monthly-resolved, year-2000 BC aerosol mass deposition rates that
158 were used in the 20th century integrations of CCSM4 that were submitted to CMIP5.
159 These deposition fluxes themselves come from a separate prognostic model
160 simulation (Lamarque et al, 2010) and are interpolated from monthly input fields
161 (as shown in Figure 1 for two model gridboxes in Greenland corresponding to
162 research camps where BC in snow has been measured in snow pits and ice cores).
163 CESM1/CAM4/CLM4 prescribed-aerosol runs were done for 10 years at two-degree
164 spatial resolution and at daily temporal resolution using repeating year-2000
165 prescribed aerosols and year-2000 greenhouse gases. The prognostic-aerosol runs
166 are from the CESM1/CAM5/CLM4 Large Ensemble Community Project (Kay et al.,
167 2014; www2.cesm.ucar.edu/models/experiments/LENS). Under this project, 30
168 realizations of CESM1 were run at 1° resolution from 1920-2100 with small
169 initialization differences for each run (Kay et al., 2014). Aerosol emissions were very
170 similar to those used by Lamarque et al. (2010) to generate the aerosol deposition
171 fields used in our prescribed-aerosol runs. In both the prescribed- and prognostic-
172 aerosol runs, in-snow processes such as melting and sublimation also affect
173 snowpack BC mixing ratios, and feedbacks amplify these effects. Output of aerosol
174 and precipitation variables from the prognostic-aerosol runs is provided at
175 monthly-average resolution only, so for this comparison we use monthly means for
176 year 2000 from all 30 members and compare it with monthly means of the
177 prescribed-aerosol run.
178 Below we compare surface snow BC mixing ratios from CESM prescribed-
179 aerosol and prognostic-aerosol runs to see if there is a systematic difference
180 between the two, despite the aerosols deriving from the same emissions year and

nearly the same emissions data base. In the model, the mixing ratio of BC in the surface snow layer (MR_{BC}) at each timestep *n* is determined by the addition of BC through dry deposition ($BCdep_{dry}$) and wet deposition ($BCdep_{wet}$) and by the addition of snow in new snowfall ($SWE_{snowfall}$). In the "real world", wet-deposited BC is added only with new snow, in the form of the mixing ratio of BC in snowfall ($MR_{BC,snowfall}$). The prognostic aerosol runs is much like the real world, while in the prescribed aerosol run, $BCdep_{wet}$ is decoupled from $SWE_{snowfall}$. Since the sum of a series of ratios ($MR_{BC,snowfall}$) does not equal the ratio of a series of sums (total $BCdep_{wet}$ and total $SWE_{snowfall}$), we expect this decoupling of deposition and snowfall will lead to errors in MR_{BC}. In addition, if there is a large amount of new snowfall, $MR_{BC,snowfall}$ will be anomalously low, but much of this low-mixing-ratio snow will be buried in the snowpack where less (or no) sunlight interacts with it. In contrast, if there is only a small amount of new snowfall, $MR_{BC,snowfall}$ will be anomalously high, and this high-mixing-ratio snow will be near the snow surface and interact with sunlight. In a model with multiple snow layers that are divided with snow accumulation, the mixing ratio in the top-most model snow layer will thus be biased high. The magnitude of the high bias will depend on the model's top snow layer thickness. In this way, low snowfall/high $MR_{BC,snowfall}$ precipitation events will have a greater influence on time-averaged snow albedo than high snowfall/low $MR_{BC,snowfall}$ precipitation events.

In addition to differences deriving from coupled versus uncoupled $BCdep_{wet}$ and $SWE_{snowfall}$, the comparison of prescribed-aerosol and prognostic-aerosol runs will be affected by other model differences, such as the simulated geographic and temporal distribution of snow cover and BC transport and scavenging in CAM5 (prognostic aerosol runs) vs. CAM4 (prescribed aerosol runs). Positive feedbacks (e.g. consolidation of BC in surface snow during snow-melt) are included in both runs, so any resulting differences in surface snow BC mixing ratios will be amplified. Therefore, we also conducted a series of offline calculations to isolate the effect of BC deposition being decoupled from snowfall rates in the prescribed runs (Table 1).

In CESM1, at each time-step, n, surface snow BC mixing ratios, $[MR_{BC}^{n}]_{,model}$ (e.g., ng g^{-1}), are determined by the dry- and wet-deposited masses of BC ($BCdep_{dry}^{n}$ and $BCdep_{wet}^{n}$; e.g. ng m^{-2}), the mass of snow in the surface snow layer (SWE_{surf}^{n}; e.g. g m^{-2}), the mixing ratio of BC from the previous time-step ($[MR_{BC}^{n-1}]_{model}$; e.g. ng g^{-1}), the fraction of the surface snow layer that is replaced by new snowfall, f_n, (once the surface snow layer has reached its maximum thickness), and the combined effects of melt and sublimation on BC and snow-water masses in the surface layer, which we will simply denote here as X (e.g. ng g^{-1}):

$$[MR_{BC}^{n}]_{model} = \frac{BCdep_{dry}^{n}}{SWE_{surf}^{n}} + \frac{BCdep_{wet}^{n}}{SWE_{surf}^{n}} + \left(1 - f_n\right)\times[MR_{BC}^{n-1}]_{model} + X, \qquad [1]$$

where:

$$f_n = {SWE_{snowfall}^{n}}\Big/{SWE_{surf}^{n}}. \qquad [2]$$

In Equation [1], the surface snow BC mixing ratio at time-step n equals the sum of, respectively, dry-deposited BC during time-step n, the addition of wet-deposited BC during time-step n, the mass of BC and snow water remaining in the surface layer at time-step n from time-step (n-1), and the impact of melt and sublimation on BC and snow water content. By definition, in prognostic-aerosol runs $BCdep_{wet}^{n}$ is zero if there is no precipitation (f_n=0), so the second term in Eqn. 1 is zero. However, in prescribed-aerosol runs there is both dry and wet BC deposition at every time-step (e.g. see Figure 1), even when there is no precipitation. Effectively this means that in prescribed-aerosol runs the mixing ratio of BC in snowfall, $MR_{BC,snowfall}^{n}$, approaches infinity as snowfall approaches zero, since:

$$MR_{BC,snowfall}^{n} = {BCdep_{wet}^{n}}\Big/{SWE_{snowfall}^{n}}. \qquad [3]$$

In our offline calculations we diagnose the BC mixing ratio both in snowfall ($MR_{BC,snowfall}^{n}$) and in our model's surface snow layer (MR_{BC}^{n}). In CLM4, the surface snow layer is of variable thickness but is always between 1cm and 3cm and is 1-2cm when snow depth exceeds 3cm (Oleson et al., 2010). In our calculations we set the surface snow layer BC mixing ratio on day 1 to that from day 1 in the prescribed-aerosol CESM1/CAM4/CLM4 run. The surface snow layer BC mixing ratios for all

subsequent days in the year are then calculated offline. Values of $BCdep^n_{dry}$, $BCdep^n_{wet}$, SWE^n_{surf} and $SWE^n_{snowfall}$ for each time-step and gridbox are taken directly from the prescribed-aerosol run of CESM1-CAM4. In our first set of offline calculations, we calculate surface snow mixing ratios that are equivalent to those from the prescribed-aerosol run, minus the effects of melting and sublimation:

$$[MR^n_{BC}]_d = \frac{BCdep^n_{dry}}{SWE^n_{surf}} + \frac{BCdep^n_{wet}}{SWE^n_{surf}} + (1 - f_n)\times[MR^{n-1}_{BC}]_d \quad [4]$$

If f_n is greater than 1.0, the surface snow layer from time-step n-1 will be buried to the second (or deeper) layers and will play no role in determining the surface snow layer BC mixing ratio. Thus, if f_n is greater than 1.0 we simply set f_n=1.0. All calculations are done at daily resolution. By not including the effects encompassed by X (Eqn. [1]) in our offline calculations we are isolating how dry and wet deposition only affect MR_{BC}. While the focus here is on BC, the same conclusions would apply for deposition/surface snow mixing ratios of dust and organic aerosols.

While Equations [1] and [4] allow for wet deposition of BC even in the absence of snowfall, a more physically realistic calculation of surface snow BC mixing ratios (minus the influence of in-snow processes) is given by:

$$MR^n_{BC} = {BCdep^n_{dry}}\Big/{SWE^n_{surf}} + f_n\times MR^n_{BC,snowfall} + (1 - f_n)\times MR^{n-1}_{BC} \quad [5]$$

In this calculation, the contribution of wet deposition to MR^n_{BC} is through the mixing ratio of BC in snowfall ($MR^n_{BC,snowfall}$), and this contribution goes to zero when the snowfall (f_n) goes to zero. However, we can not use in Eqn. [5] $MR^n_{BC,snowfall}$ as calculated directly from $BCdep^n_{wet}$ and $SWE^n_{snowfall}$ from the prescribed-aerosol run, since , as noted above, this sometimes yields infinite values of $MR^n_{BC,snowfall}$. Therefore, we re-calculate $MR^n_{BC,snowfall}$ by assuming that total BC mass deposition flux scales with total snowfall (in snow water equivalent) within each month and gridbox, yielding the smoothed values $[MR_{BC,snowfall}]_m$ and $[MR_{BC,snowfall}]_y$, which are calculated as follows:

$[MR_{BC,snowfall}]_m$: Within each month of the multi-year model run, $SWE_{snowfall}$ and $BCdep_{wet}$ from the prescribed-aerosol model run are summed. Monthly

values of $MR_{BC,snowfall}$ are calculated from the ratio of the monthly-total $BCdep_{wet}$ and monthly-total $SWE_{snowfall}$.

$[MR_{BC,snowfall}]_y$: A monthly climatology of monthly-total $SWE_{snowfall}$ is computed. Monthly values of $MR_{BC,snowfall}$ are calculated from the ratio of the monthly-total $BCdep_{wet}$ and the monthly climatology of $SWE_{snowfall}$.

These smoothed snowfall BC mixing ratios are compared to those given by using the prescribed-aerosol model values directly:

$[MR_{BC,snowfall}]_d$: Each day $MR_{BC,snowfall}$ is calculated as the ratio of the prescribed daily $BCdep_{wet}$ (e.g. Figure 1) and daily $SWE_{snowfall}$.

The wet and dry BC mass deposition rates used to calculate all values of $\boldsymbol{MR}^n_{BC,snowfall}$ are exactly those used in the prescribed-aerosol runs. The total BC mass and total snow mass deposited to the surface within a given month and gridbox, averaged across all years, is the same across all three sets of these calculations, so the only difference in how they affect surface snow BC mixing ratios is through the relative timing of BC versus snow deposition to the surface.

Surface snow BC mixing ratios $[MR_{BC}]_d$ for each gridbox/day are then calculated using Equation [4], and corresponding values of $[MR_{BC}]_m$ and $[MR_{BC}]_y$ are calculated using Equation [5] and $[MR_{BC,snowfall}]_m$ and $[MR_{BC,snowfall}]_y$, respectively (Table 1). We again emphasize that the values $[MR_{BC}]_d$ are analogous to those in CESM1 when aerosol deposition fluxes are prescribed, minus the effects of melt and sublimation; i.e., time-averaged, smoothed prescribed $BCdep_{wet}$ is paired with daily-varying $SWE_{snowfall}$, and wet deposition is present even when there is zero new snowfall. In contrast, $[MR_{BC,snowfall}]_m$ and $[MR_{BC,snowfall}]_y$ use $SWE_{snowfall}$ values that have been increasingly time-averaged, and so are more physically consistent with $BCdep_{wet}$, which is the product of averaging across multiple prognostic model run years. Further, $[MR_{BC}]_m$ and $[MR_{BC}]_y$ are only affected by wet deposition when there is new snowfall.

We conduct two full sets of offline calculations of $[MR_{BC,snowfall}]_d$, $[MR_{BC,snowfall}]_m$, $[MR_{BC,snowfall}]_y$ and $[MR_{BC}]_d$, $[MR_{BC}]_m$,$[MR_{BC}]_y$ (Table 1). In one set of offline calculations, $\boldsymbol{MR}^n_{BC,snowfall}$ and f_n are calculated using $SWE_{snowfall}$ taken

296 directly from our prescribed-aerosol model runs; we will refer to these as the
297 "CESMmet" (CESM meteorology) calculations. In a second set of calculations, model
298 snowfall rates were replaced with CRU/NCEP reanalysis daily precipitation for
299 years 2004-2009 in order to mimic the runs reported by Jiao et al. (2014); we will
300 refer to these as the "CRUNCEPmet" calculations. The CRU/NCEP data set specifies
301 precipitation rates but not whether it is rain or snow, so we made the simple
302 assumption that when the reported surface air temperature was 0°C or lower the
303 precipitation was snowfall. In both cases, snow cover – specifically, the snow water
304 equivalent in the surface snow layer for each day and gridbox – is the average across
305 the 10 model years of the year-2000 CESM1-CAM4 run. Calculations are done for all
306 variables for either 10 years, using $SWE_{snowfall}$ values from the model (CESMmet;
307 repeating year 2000 meteorology) or 6 years, using $SWE_{snowfall}$ from the CRU/NCEP
308 reanalysis data set (CRUNCEPmet; years 2004-2009 meteorology).
309 Note that while averaged values of $SWE_{snowfall}$ were used to calculate
310 $[MR_{BC,snowfall}]_m$ and $[MR_{BC,snowfall}]_y$, the fraction of surface snow replaced by new
311 snowfall (f_n) is always calculated using the daily-varying value of $SWE_{snowfall}$ from
312 either CESM1-CAM4 (CESMmet) or the CRU/NCEP reanalysis data set
313 (CRUNCEPmet). In other words, the rate of snowfall varies daily according to the
314 model (CESMmet) or reanalysis (CRUNCEPmet) meteorology in all offline
315 calculations, but the BC mixing ratio in that snowfall is either $[MR_{BC,snowfall}]_d$,
316 $[MR_{BC,snowfall}]_m$ or $[MR_{BC,snowfall}]_y$. This allows for realistic evolution of the snowpack
317 water mass while testing the effect of using different estimates of the mass mixing
318 ratio of BC in snowfall.
319 We compare the results of the prognostic-aerosol runs versus the
320 prescribed-aerosol runs and across our six sets of offline calculations (Table 1) for
321 three geographic regions where forcing by BC in snow on land is climatically
322 important: Greenland (60°-85°N, 290°-340°W) North America (50°-80°N, 190°-
323 300°W) and Eurasia (60°-75°N, 30°-180°W). Only those gridboxes containing snow
324 on land are included in the statistics presented below; snowfall on sea ice and BC in
325 snow on sea ice are not considered here.

Results

Prescribed runs vs. prognostic runs

Differences in the meteorology and in aerosol transport and scavenging rates between the prognostic-aerosol and prescribed-aerosol runs lead to differences in the average mass of deposited BC ($BC_{dep,wet}$+$BC_{dep,dry}$) and in the average snowfall snow water mass ($SWE_{snowfall}$) within each region (Table 2). The BC deposition fluxes and mixing ratios in the surface snow are considerably higher in the prescribed runs compared to the prognostic runs. However, the greater values of MR_{BC} in each region for the prognostic-aerosol runs exceed a simple estimate of how MR_{BC} is expected to change based on scaling the relative changes in $BC_{dep,wet}$+$BC_{dep,dry}$ by the relative changes in $SWE_{snowfall}$. This indicates that MR_{BC} is exaggerated in the prescribed run by other model differences. Scaling for the relative changes in BC and snow water deposition, we estimate that MR_{BC} is a factor of 3.1, 1.7 and 1.6 higher in in Greenland, Eurasia and North America, respectively, in the prescribed-aerosol runs than in the prognostic-aerosol runs due to model differences other than changes in BC deposition and snowfall rates. Both runs include the effects of melt and sublimation, so their differences in MR_{BC} have been amplified, since these processes have positive feedbacks to MR_{BC}. While we have scaled to account for differences in total BC deposition and snowfall between the two models, the spatial and temporal distributions of deposited BC and snowfall, and how the two correlate, will also likely differ, with impacts on both $MR_{BC,snowfall}$ and MR_{BC}. Ideally we would be able to compare daily BC deposition and snowfall (and therefore $MR_{BC,snowfall}$) within each gridbox from both the prescribed-aerosol and prognostic-aerosol runs. Unfortunately, BC wet deposition in snow and rain are not distinguished in the output of the prognostic run ensembles. Thus, we are unable to further isolate the source of the differences in the prescribed- and prognostic-aerosol surface snow BC mixing ratios.

A similar comparison between paired prescribed-aerosol and prognostic-aerosol CESM runs was described briefly by Jiao et al. (2014), and our analysis of

their runs provides additional confirmation of a systematic difference between prescribed- and prognostic-aerosol runs. One simulation involved CAM4 and CLM4 coupled with prognostic aerosol deposition, i.e., with self-consistent meteorology and deposition. The other simulation was conducted with CLM in stand-alone mode, driven with 6-hourly CRU/NCEP meteorology and with monthly-averaged prescribed BC deposition fluxes from the first run. We analyzed Jiao et al.'s runs and found that the annual northern hemisphere average concentration of BC in the surface snow layer was larger by a factor of 2.0 in the prescribed-aerosol simulation, weighted by snow-covered area in each month and averaged over the same domains, despite the fact that time-averaged BC deposition fluxes were identical in both simulations. Our analysis of Jiao's et al.'s runs therefore supports the main conclusions drawn earlier from comparing prescribed- and prognostic-aerosol runs above. Our offline calculations provide further support to our hypothesis that the prescribed-aerosol runs will have a high bias in surface snow BC mixing ratios due to the fact that BC and snow water deposition to the surface are decoupled in the prescribed runs.

Offline calculations

Our offline-calculated snowfall BC mixing ratio, $[MR_{BC,snowfall}]_d$, which simulates the mixing ratio of BC in snowfall in the prescribed-aerosol runs, is extremely variable (Figure 2a), because $BCdep_{wet}$ is smoothly varying (Figure 1) but snowfall is episodic. $[MR_{BC,snowfall}]_d$ computed with snowfall from the CRUNCEPmet data (not shown) are similarly variable. If snowfall on a particular day approaches zero, $[MR_{BC,snowfall}]_d$ approaches infinity (i.e. why we are unable to provide a mean in Figure 2a), though f_n simultaneously approaches zero. Conversely, heavier snowfall events are associated with anomalously low values of $[MR_{BC,snowfall}]_d$. $[MR_{BC,snowfall}]_m$ is dramatically lower and less variable but still covers a significant range (Figure 2b). When the smooth values of $BCdep_{wet}$ (Figure 1) are combined with a 10-year monthly snowfall climatology the mixing ratios of BC in snowfall, $[MR_{BC,snowfall}]_y$ (Figure 2c), become much less variable and, importantly, systematically lower.

As noted above, our offline calculations of $[MR_{BC}]_d$ are intended to approximate the CESM1-CAM4 prognostic-aerosol model runs, minus the effects of sublimation and snowmelt on MR_{BC}. In Figure 3 we show that the difference in the offline-calculated $[MR_{BC}]_d$ values and the CESM1-CAM4 values of the surface snow BC mixing ratio, $[MR_{BC}]_{prescr}$, are small relative to the overall variability in MR_{BC}, except when there is surface snow melt (e.g. percolation and ablation zones glaciers such as the Greenland site shown in Figure 3a, and during the spring for seasonal snow, such as around day 150 for the Eurasian gridbox shown in Figure 3b). The small differences outside of the melt season indicate that we can use our offline values of $[MR_{BC}]_d$ as a proxy for $[MR_{BC}]_{prescr}$ in comparisons to $[MR_{BC}]_m$ and $[MR_{BC}]_y$ in order to understand the effects on MR_{BC} of using decoupled BC and snowfall deposition.

Surface snow BC mixing ratios become smaller as the wet deposition flux of BC varies in a more physically consistent way with snowfall, i.e. going from $[MR_{BC}]_d$ to $[MR_{BC}]_m$ to $[MR_{BC}]_y$ (Table 3, and Figures 3-5), even though the total mass of BC and snow deposited doesn't change. The values in Figure 3 are examples for just one gridbox each in Greenland and Eurasia, two regions that account for a large fraction of Arctic spring and summer forcing by BC in snow in CESM1/CAM4/CLM4 runs (see Fig. 5 of Goldenson et al., 2012). Table 3 gives annual averages, medians and standard deviations of $[MR_{BC}]_d$, $[MR_{BC}]_m$, and $[MR_{BC}]_y$ for all gridbox/days in our three study regions, as well as the median and snowfall-weighted mean of $[MR_{BC,snowfall}]_d$, $[MR_{BC,snowfall}]_m$, and $[MR_{BC,snowfall}]_y$. The median of $[MR_{BC,snowfall}]_d$ is much higher than the median of $[MR_{BC,snowfall}]_m$ and $[MR_{BC,snowfall}]_y$ because, as noted above, as snowfall approaches zero $[MR_{BC,snowfall}]_d$ approaches infinity. Weighting $MR_{BC,snowfall}$ by snowfall amount provides a better metric for its influence on surface snow BC mixing ratios. In the weighted averages, $[MR_{BC,snowfall}]_d$ is actually lower than $[MR_{BC,snowfall}]_m$, and $[MR_{BC,snowfall}]_y$. This is because the mass of BC wet-deposited on days with zero snowfall (when $[MR_{BC,snowfall}]_d$ is infinity) is not counted in the snowfall-weighted mean. However, this mass does contribute $[MR_{BC}]_d$, since in this calculation BC mass flux to the surface is independent of snowfall and, as argued above, the high-$MR_{BC,snowfall}$/low-$SWE_{snowfall}$ events have a greater impact on the

418 surface snow layer BC mixing ratios than do the low-$MR_{BC,snowfall}$/high-$SWE_{snowfall}$
419 events. The net result is that the mean and median of $[MR_{BC}]_d$ is higher than
420 $[MR_{BC}]_m$ and $[MR_{BC}]_y$ in all three regions (Table 3).
421 Figures 4 and 5 show histograms of the ratio $[MR_{BC}]_d$:$[MR_{BC}]_y$ for winter,
422 spring and (Greenland only) summer from all gridboxes in Greenland, Eurasia and
423 North America. These ratios are shown using both CESMmet (Fig. 4) and
424 CRUNECPmet (Fig. 5). Maps of seasonal averages of these ratios using CESMmet are
425 shown in Supplemental Figures S1-S3. It is apparent that decoupling BC deposition
426 and the snowfall that should be driving that deposition leads to high biases in
427 surface snow BC mixing ratios of, on average, a factor of 1.5-1.6 in N. America and
428 Eurasia and 2.2-2.5 in Greenland (Table 4). In other words, when CESM is run in
429 prescribed aerosol mode, the seasonally-averaged daily surface snow BC mixing
430 ratios will, on average, be on the order of 1.5-2.5 times higher than they would be if
431 BC deposition scaled with snowfall. This difference is notably consistent with the
432 finding above that regionally-averaged surface snow BC mixing ratios in the
433 prescribed-aerosol runs were a factor of 1.6-3.0 higher than in the prognostic-
434 aerosol runs. The somewhat higher difference in the model runs may be due to the
435 fact that they include the effects of melt and sublimation, since the positive
436 feedbacks between MR_{BC} and snow melt and sublimation would lead to
437 amplification of any high biases. While our emphasis is on the annual-average bias
438 over broad regions, within a given day or gridbox the biases can be lower (in some
439 cases <1.0) or higher than this, with significant implications for comparisons of
440 observed and modeled MR_{BC} at given locations/times.
441 As noted earlier, prescribed-aerosol wet deposition fluxes are based on
442 prognostic model runs and so are influenced by the prognostic model's precipitation
443 rates. Biases in the prognostic model's precipitation rates at a given location will
444 therefore translate directly to biases in the aerosol mass deposition rates. Coupling
445 these model-derived BC mass deposition rates with observed precipitation rates can
446 therefore produce unrealistic values of MR_{BC} both 1) where there are systematic
447 biases in the prognostic model's snowfall and 2) where the inter-annual variability
448 in the model is decoupled from the observed snowfall rates used in the prescribed-

aerosol run or offline calculation (i.e., here, year 2000 of a prognostic aerosol model vs. 2004-2009 of CRU/NCEP). Thus, using reanalysis data for snowfall rates in offline estimates of BC albedo forcing such as those conducted for ACCMIP (Lee et al., 2013) may introduce an additional source of bias in MR_{BC}.

Our offline values of $[MR_{BC}]_d$ calculated using the CRUNCEPmet snowfall rates are analogous to those in the "NCAR-CAM3.5" year 2000 results of Lee et al. (2013; see their Table 1), as both use year-2000 prescribed BC mass deposition fluxes as described by Lamarque et al. (2013) and year 2004-2009 CRU/NCEP reanalysis precipitation. In Table 3 we show the seasonally-averaged ratios $[MR_{BC}]_d$:$[MR_{BC}]_y$ for the CRUNCEPmet calculations. These ratios include the effects of using the physically inconsistent daily BC deposition and snowfall rates (i.e. $[MR_{BC,snowfall}]_d$) versus using the more physically consistent "climatological" BC deposition and snowfall rates (i.e. $[MR_{BC,snowfall}]_y$) and they include the effect of any differences between the model year-2000 snowfall and reanalysis 2004-2009 snowfall. The net effect is that the ratios $[MR_{BC}]_d$:$[MR_{BC}]_y$ are somewhat lower (Table 3) when using reanalysis snowfall (CRUNCEPmet) than when using model snowfall (CESMmet), indicating that differences in model vs. reanalysis snowfall are compensating for some of the bias seen in the ratios from the CESMmet calculations. However, ratios are also much more variable (i.e. Figure 5 vs Figure 4). Again, this has implications for comparisons of prescribed aerosol model MR_{BC} values with observed surface snow BC mixing ratios from specific locations and time periods, as was done by Goldenson et al. (2012) and Jiao et al. (2014).

Since the prescribed BC mass deposition fluxes used in the model runs are spatially-smoothed climatologies, we consider coupling these deposition fluxes with climatological snowfall rates to provide a more realistic estimate of how BC wet deposition affects time-averaged surface snow BC mixing ratios. Further, we have shown that doing so yields lower surface snow BC mixing ratios, and so assert that prescribed-aerosol runs of CESM1 include a high bias. The ratios $[MR_{BC}]_d$:$[MR_{BC}]_y$ provide a first-order estimate of this bias. Note that this bias is in addition to any other inherent model biases, e.g. in emissions, transport and scavenging rates, some of which may offset each other. Thus, correcting for this bias may not yield better

agreement with observations; if this is the case, this simply means there are other sources of bias that also must be corrected.

Discussion and Conclusions

We argue that prescribing temporally- and geographically-smoothed surface BC deposition fluxes in a model where snowfall varies on typical meteorological timescales (i.e., daily or faster) will produce high biases in time-averaged surface snow BC mixing ratios. Using comparisons of prescribed-aerosol and prognostic-aerosol model runs and offline calculations we have demonstrated that: a) Prescribed-aerosol runs have higher surface snow BC mixing ratios than prognostic-aerosol runs, by a factor of about 1.6-3.0, despite being based on the same BC emissions and accounting to first order for differences in total BC and snow deposited to the surface, and b) Decoupling of BC wet deposition fluxes and snowfall rates leads to surface snow BC mixing ratios a factor of about 1.5-2.5 higher than if the same mass of BC was wet- deposited in proportion to the snowfall snow mass. Both of these biases are significant at daily, seasonal and annual timescales.

Black carbon mass deposition fluxes in snowfall depend on ambient BC concentrations, the scavenging efficiency of BC in snow, and snowfall rates. Thus, while BC deposition fluxes do not depend solely on precipitation rates, removing any dependence on snowfall leads to biases in the mixing ratio of BC in snowfall, $MR_{BC,snowfall}$. If BC deposition rates and snowfall rates are fully decoupled, $MR_{BC,snowfall}$ will be biased high on days of lower snowfall, when the fractional contribution to surface snow (f_n) is lower than average. Conversely, $MR_{BC,snowfall}$ will be biased low on days when f_n is higher than average. As our offline calculations have shown, this anti-correlation between deviations in $MR_{BC,snowfall}$ and in f_n from their averages does not mean that low and high biases in $MR_{BC,snowfall}$ have offsetting effects on surface snow BC mixing ratios (MR_{BC}). This is because the cases of high-biased $MR_{BC,snowfall}$ remain near the snow surface so they have a strong influence on MR_{BC}. Conversely, cases of low-biased $MR_{BC,snowfall}$ may contribute to snow deeper in the snowpack and so have less influence on the surface snow BC mixing ratio.

We estimate that prescribed aerosol model runs of CESM1 have approximately a factor of 1.5-2.5 high bias in surface snow BC mixing ratios due to the use of climatological/smoothed BC mass deposition fluxes coupled with modeled, daily-varying snowfall. In CESM1 (i.e. in the SNICAR component of CLM) the surface snow layer is 1-3cm deep. Sunlight usually can penetrate >10cm into the snowpack, depending on snow density (Warren and Wiscombe, 1980), so mixing ratios over this full depth are relevant for albedo reduction and BC albedo forcing. SNICAR accounts for this, with albedo being determined by MR_{BC} in as many snow layers as is reached by sunlight (typically the top 2-3 layers). We expect the bias in surface snow BC mixing ratios will decrease as the depth of the top snow layer increases, becoming zero as the depth of the surface layer approaches the total snowpack depth. When multiple layers are represented, the high biases in BC mixing ratios in the surface layer will be accompanied by low biases in BC mixing ratios in deeper snow layers. However, since the amount of sunlight drops off rapidly with snow depth MR_{BC} in the top few cm of the snowpack has the strongest influence on albedo and most absorption of sunlight will occur in the top few cm of the snowpack, i.e. the surface snow layer in SNICAR. It is beyond the scope of this study to calculate the exact impact on modeled albedo for snow of different densities and therefore different sunlight penetration depths. It is sufficient to point out that:

a) Using climatological, prescribed mass deposition fluxes coupled with daily precipitation rates produces a large positive bias in surface snow BC mixing ratios (MR_{BC}) that is significant across daily, seasonal and annual-average time-scales and at gridbox to broad regional (and therefore also global) geographic scales;

b) Existing studies using CESM1 and prescribed aerosols to study BC albedo forcing (e.g. Goldenson et al., 2012; Holland et al, 2012; Lawrence et al, 2012; Lee et al., 2013; and Jiao et al., 2014; and all CMIP5 integrations with CCSM4) are biased by this effect;

c) An alternate approach should be used in CESM to calculate surface snow mixing ratios of BC and other particulate absorbers. This also applies to any

other model using or planning to use prescribed wet deposition fluxes to study the climate impact of albedo forcing.

While the examples shown here are all for higher latitude northern regions, BC albedo forcing has also been hypothesized to have a significant effect on climate and snow cover in the Himalayan and Tibetan Plateau (e.g. Xu et al., 2009; Qian et al., 2011; Xu et al., 2012). Accurate representation of snowfall rates in this region are particularly challenging for climate models; e.g. see Figure 2 of Qian et al., 2011, which shows a significant positive biases in snow cover over the Tibetan plateau when using CAM3.1. These biases in modeled snow cover directly affect modeled BC albedo forcing, including in model runs with prognostic aerosols, since this forcing is zero anywhere with no snow. In addition, if modeled snowfall in this region is systematically biased high, as appears likely to be the case in CESM1 for the Tibetan Plateau, prescribed BC wet deposition mass fluxes based on prognostic runs of this model are also likely biased high. When coupled with more realistic snowfall rates such as from reanalysis data (e.g. as done by Lee et al., 2013; Jiao et al., 2014), this will produce overall high biases in MR_{BC} in this region.

We suggest that, for wet deposition, one option is that instead of prescribing mass deposition fluxes (e.g. kg m^{-2} sec^{-1} BC deposition) the model could instead prescribe mass mixing ratios in snowfall (e.g. ng BC per g snowfall SWE, or ppb BC per snowfall water). These prescribed mass mixing ratios could be a climatology from a multi-year integration of a prognostic aerosol model. The appropriate number of model run years would need to be determined by testing how both the mean and variability in snow mixing ratios change with number of years averaged. Aerosol dry deposition will need to continue to be prescribed as a mass flux since it does not scale with snowfall. The value of MR_{BC} at timestep n could then be calculated directly as given in Equation [5], as used here in our offline calculations of $[MR_{BC}]_m$ and $[MR_{BC}]_y$. While this will produce an inconsistency in the mass balance of BC within the prescribed model runs (i.e. the change with time in the mass of BC in the atmosphere will not equal BC minus BC deposited to the surface within the prescribed–aerosol runs), both the atmospheric BC concentrations and surface snow BC mixing ratios in the model calculation will be physically more consistent.

572 This is preferable to maintaining mass balance within the prescribed-aerosol run
573 since both the atmospheric concentrations and deposition rates are anyhow
574 prescribed, and the climatically important variable in studies of albedo forcing is the
575 surface snow BC mixing ratio.
576
577 **Acknowledgements**
578 This study was supported by the National Science Foundation grant ARC-1049002.
579 We thank C. Jiao for helpful analysis of model simulations. We also thank two
580 reviewers for suggestions that lead to significant improvement to the paper.
581
582

583 **References**

584

585 Bond, T. C., S. J. Doherty, D. W. Fahey, P. M. Forster, T. Berntsen, B. J. DeAngelo, M. G.
586 Flanner, S. Ghan, B. Kärcher, D. Koch, S. Kinne, Y. Kondo, P. K. Quinn, M. C.
587 Sarofim, M. G. Schultz, M. Schulz, C. Venkataraman, H. Zhang, S. Zhang, N.
588 Bellouin, S. K. Guttikunda, P. K. Hopke, M. Z. Jacobon, J. W. Kaiser, Z. Klimont, U.
589 Lohmann, J. P. Schwarz, D. Shindell, T. Storelvmo, S. G. Warren and C. S. Zender,
590 Bounding the Role of Black Carbon in Climate: A scientific assessment, J.
591 Geophys. Res., 118(11), 5380-5552, doi:10.1002/jgrd.50171, 2013.
592 Boucher, O., D. Randall, P. Artaxo, C. Bretherton, G. Feingold, P. Forster, V.-M.
593 Kerminen, Y. Kondo, H. Liao, U. Lohmann, P. Rasch, S.K. Satheesh, S. Sherwood, B.
594 Stevens and X.Y. Zhang, Clouds and Aerosols. In: Climate Change 2013: The
595 Physical Science Basis. Contribution of Working Group I to the Fifth Assessment
596 Report of the Intergovernmental Panel on Climate Change [Stocker, T.F., D. Qin,
597 G.-K. Plattner, M. Tignor, S.K. Allen, J. Boschung, A. Nauels, Y. Xia, V. Bex and P.M.
598 Midgley (eds.)]. Cambridge University Press, Cambridge, United Kingdom and
599 New York, NY, USA, 2013.
600 Conway, H., A. Gades, and C. F. Raymond, Albedo of dirty snow during conditions of
601 melt, Water Resour. Res., 32(6), 1713–1718, 1996.
602 Doherty, S. J., T. C. Grenfell, S. Forsström, D. L. Hegg, S. G. Warren and R. Brandt,
603 Observed vertical redistribution of black carbon and other light-absorbing
604 particles in melting snow, J. Geophys. Res., 118(11), 5553-5569,
605 doi:10.1002/jgrd.50235, 2013.
606 Doherty, S. J., S. G. Warren, T. C. Grenfell, A. D. Clarke, R. Brandt, Light-absorbing
607 impurities in Arctic snow, Atmos. Chem. Phys., 10, 11647-11680,
608 doi:10.5294/acp-10-11647-2010, 2010.
609 Flanner, M. G., C. S. Zender, P. G. Hess, N. M. Mahowald, T. H. Painter, V. Ramanathan,
610 and P. J. Rasch, Springtime warming and reduced snow cover from carbonaceous
611 particles, Atmos. Chem. Phys., 9(7), 2481–2497, doi:10.5194/acp-9-2481-2009,
612 2009.

613 Flanner, M. G., C. S. Zender, J. T. Randerson, and P. J. Rasch, Present-day climate
614 forcing and response from black carbon in snow, J. Geophys. Res., 112(D11), 202,
615 doi:10.1029/2006JD008003, 2007.
616 Forsström, S., E. Isaksson, R. B. Skeie, J. Ström, C. A. Pedersen, S. R. Hudson, T. K.
617 Berntsen, H. Lihavainen, F. Godtliebsen and S. Gerland, Elemental carbon
618 measurements in European Arctic snow packs, J. Geophys. Res., 118, 13614-
619 13627, doi:10.1022/2013JD019886, 2013.
620 Goldenson, N., S. J. Doherty, C. M. Bitz, M. M. Holland, B. Light, and A. J. Conley, Arctic
621 climate response to forcing from light-absorbing particles in snow and sea ice in
622 CESM, Atmos. Chem. Phys., 12, 7903-7920, doi:10.5194/acp-12-7903-2012,
623 2012.
624 Hansen, J., and L. Nazarenko, Soot climate forcing via snow and ice albedos, P. Natl.
625 Acad. Sci. USA, 101(2), 423–428, doi:10.1073/pnas.2237157100, 2004.
626 Holland, M., Bailey, D. A., Briegleb, B. P., Light, B., and Hunke, E.: Improved sea ice
627 shortwave radiation physics in CCSM4: the impact of melt ponds and aerosols on
628 Arctic sea ice, J. Climate, 25, 1413–1430, doi:10.1175/JCLI-D-11-00078.1, 2012.
629 Jacobson, M. Z., Climate response of fossil fuel and biofuel soot, accounting for soot's
630 feedback to snow and sea ice albedo and emissivity, J. Geophys. Res., 109(D21),
631 D21201, doi:10.1029/2004JD004945, 2004.
632 Jiao, C., M. G. Flanner, Y. Balkanski, S. E. Bauer, N. Bellouin, T. K. Berntsen, H. Bian, K.
633 S. Carslaw, M. Chin, N. de Luca, T. Diehl, S. J. Ghan, T. Iversen, A. Kirkevåg, D.
634 Koch, X. Liu, G. W. Mann, J. E. Penner, G. Pitari, M. Schulz, Ø . Seland, R. B. Skeie, S.
635 D. Steenrod, P. Stier, T. Takemura, K. Tsigaridis, T. van Noije, Y. Yun and K. Zhang,
636 An AeroCom assessment of black carbon in Arctic snow and sea ice, Atmos.
637 Chem. Phys., 14, 2399-2417, doi:10.5194/acp-14-2399-2014, 2014.
638 Kay, J. E., C. Deser, A. Phillips, A. Mai, C. Hannay, G. Strand, J. Arblaster, S. Bates, G.
639 Danabsoglu, J. Edwards, M. Holland, P. Kushner, J.-F. Lamarque, D. Lawrence, K.
640 Lindsay, A. Middleton, E. Munoz, R. Neale, K. Oleson, L. Polvani and M.
641 Vertenstein, The Community Earth System Model (CESM) Large Ensemble
642 Project: A community resource for studying climate change in the presence of
643 internal climate variability, *Bull. Amer. Met. Soc.*, submitted, 2014.

644 Koch, D., S. Menon, A. Del Genio, R. Ruedy, I. Alienov, and G. A. Schmidt,
645 Distinguishing aerosol impacts on climate over the past century,J. Climate,
646 22(10), 2659–2677, doi:10.1175/2008jcli2573.1, 2009.
647 Kopacz, M., D. L. Mauzerall, J. Wang, E. M. Leibensperger, D. K. Henze and K. Singh,
648 Origin and radiative forcing of black carbon transported to the Himalayas and
649 Tibetan Plateau, Atmos. Chem. Phys., 11, 2837-2852, doi:10.5194/acp-11-2837-
650 2011, 2011.
651 Lamarque, J.-F., D. T. Shindell, B. Josse, P. J. Young, I. Cionni, V. Eyring, D. Bergmann,
652 P. Cameron-Smith, W. J. Collins, R. Doherty, S. Dalsoren, G. Faluvegi, G. Folberth,
653 S. J. Ghan, L. W. Horowitz, Y. H. Lee, I. A. MacKenzie, T. Nagashima, V. Naik, D.
654 Plummer, M. Righi, S. T. Rumbold, M. Schulz, R. B. Skeie, D. S. Stevenson, S.
655 Strode, K. Sudo, S. Szopa, A. Voulgarakis and G. Zeng, The Atmospheric Chemistry
656 and Climate Model Intercomparison Project (ACCMIP): overview and description
657 of models, simulations and climate diagnostics, Geosci. Model Dev., 6, 179-206,
658 doi:10.5194/gmd-6-179-2013, 2013.
659 Lawrence, D. M., K. W. Oleson, M. G. Flanner, C. G. Fletcher, P. J. Lawrence, S. Levis, S.
660 C. Swenson, and G. B. Bonan, The CCSM4 Land Simulation, 1850-2005:
661 Assessment of Surface Climate and New Capabilities, J. Climate, 25,
662 doi:10.1175/JCLI-D-11-00103.1, 2012.
663 Lee, Y. H., J.-F. Lamarque, M. G. Flanner, C. Jiao, D. T. Shindell, T. Berntsen, M. M.
664 Bisiaux, J. Cao, W. J. Collins, M. Curran, R. Edwards, G. Faluvegi, S. Ghan, L. W.
665 Horowitz, J. R. McConnell, J. Ming, G. Myhre, T. Nagashima, V. Naik, S. T. Rumbold,
666 R. B. Skeie, K. Sudo, T. Takemura, F. Thevonon, B. Xu and J.-H. Yoon, Evaluation of
667 preindustrial to present-day black carbon and its albedo forcing from
668 Atmospheric Chemistry and Climate Model Intercomparison Project (ACCMIP),
669 Atmos. Chem. Phys., 13, 2607-2634, doi:10.5194/acp-13-2607-2013, 2013.
670 Oleson, K. W., D. M. Lawrence, G. B. Bonan, M. G. Flanner, E. Kluzek, P. J. Lawrence, S.
671 Levis, S. C. Swenson, P. E. Thornton, Technical Description of vserion 4.0 of the
672 Community Land Model (CLM), NCAR Technical Note NCAR/TN-478+STR, 2010.
673 Qian, Y., M. G. Flanner, L. R. Leung and W. Wang (2011), Sensitivity studies on the
674 impacts of Tibetan Plateau snowpack pollution on the Asian hydrological cycle

and monsoon climate, Atmos. Chem. Phys., 11, 1929-1948, doi:10.5194/acp-11-1929-2011, 2011.

Shindell, D.T., J.-F. Lamarque, M. Schulz, M. Flanner, C. Jiao, M. Chin, P.J. Young, Y.H. Lee, L. Rotstayn, N. Mahowald, G. Milly, G. Faluvegi, Y. Balkanski, W.J. Collins, A.J. Conley, S. Dalsoren, R. Easter, S. Ghan, L. Horowitz, X. Liu, G. Myhre, T. Nagashima, V. Naik, S.T. Rumbold, R. Skeie, K. Sudo, S. Szopa, T. Takemura, A. Voulgarakis, J.-H. Yoon, and F. Lo, Radiative forcing in the ACCMIP historical and future climate simulations. Atmos. Chem. Phys., 13, 2939-2974, doi:10.5194/acp-13-2939-2013, 2013.

Warren, S. G., and W. J. Wiscombe, A model for the spectral albedo of snow. II: Snow containing atmospheric aerosols, J. Atmos. Sci., 37(12), 2734–2745, 1980.

Xu, B., J. Cao, J. Hansen, T. Yao, D. R. Joswia, N. Wang, G. Wu, M. Wang, H. Zhao, W. Yang, X. Liu and J. He, Black soot and the survival of Tibetan glaciers, P. Natl. Acad. Sci. USA, 106, 22114-22118, doi:10.1073/pnas.0910444106, 2009.

Xu, B., J. Cao, D. R. Joswiak , X. Liu, H. Zhao and J. He, Post-depositional enrichment of black soot in snow-pack and accelerated melting of Tibetan glaciers, Environ. Res. Lett., 7, doi:10.1088/1748-9326/7/1/014022, 2012.

706 **Table 1.** Overview of the model runs and offline calculations compared herein. All
707 are based on the same year-2000 aerosol and aerosol precursor emissions dataset
708 (Lamarque et al. ,2010).

model run/ calculation type	**ensemble members**	**surf snow BC mixing ratio**	**snowfall used for $[MR_{BC}]_{snowfall}$ & f_n**
CESM1/CAM5/CLM4, prognostic	30	$[MR_{BC}]_{model,prognost}$	modeled snowfall rates
CESM1/CAM4/CLM4, prescribed	10	$[MR_{BC}]_{model,\ prescr}$	modeled snowfall rates (= "CESMmet")
offline	10	$[MR_{BC}]_d$, Eqn [4]	CESMmet
offline	10	$[MR_{BC}]_m$, Eqn [5]	CESMmet
offline	10	$[MR_{BC}]_y$, Eqn [5]	CESMmet
offline	6	$[MR_{BC}]_d$, Eqn [4]	CRUNCEPmet
offline	6	$[MR_{BC}]_m$, Eqn [5]	CRUNCEPmet
offline	6	$[MR_{BC}]_y$, Eqn [5]	CRUNCEPmet

709
710

711 **Table 2.** Annual means, medians and standard deviations of monthly-average BC
712 mass deposition (ng m^{-2} day^{-1}), snowfall in snow water equivalent (g m^{-2} day^{-1}) and
713 surface snow BC mixing ratios (ng g^{-1}) for all gridboxes in each of three study
714 regions, for the prognostic-aerosol and prescribed-aerosol model runs. Also shown
715 are the ratios of the means and medians of each.

		prognostic	prescribed	ratio of means, prescribed: prognostic
Greenland				
$BC_{dep,wet}+BC_{dep,dry}$	mean	1.50	7.2	4.80
	median	0.55	4.9	8.91
	std dev.	2.30	6.30	---
$SWE_{snowfall}$	mean	0.66	1.10	1.67
	median	0.42	0.77	1.83
	std dev.	0.92	0.83	---
MR_{BC}	mean	2.40	21.1	8.79
	median	0.76	12.0	17.11
	std dev.	4.40	21.1	---
North America				
$BC_{dep,wet}+BC_{dep,dry}$	mean	11.1	19.5	1.76
	median	4.30	13.8	3.21
	std dev.	15.0	17.2	---
$SWE_{snowfall}$	mean	0.45	0.57	1.27
	median	0.28	0.56	2.00
	std dev.	0.72	0.46	---
MR_{BC}	mean	9.90	23.1	2.33
	median	3.10	12.7	4.10
	std dev.	21.2	30.6	---
Eurasia				
$BC_{dep,wet}+BC_{dep,dry}$	mean	20.9	35.9	1.72
	median	11.6	29.1	2.51
	std dev.	24.7	28.8	---
$SWE_{snowfall}$	mean	0.54	0.63	1.17
	median	0.45	0.63	1.40
	std dev.	0.50	0.45	---
MR_{BC}	mean	20.8	48.8	2.35
	median	8.80	34.3	3.90
	std dev.	34.2	54.0	---

716

Table 3. Means, medians and standard deviations of BC mixing ratios in snowfall ($MR_{BC,snowfall}$; ng g^{-1}) and in the surface snow layer (MR_{BC}; ng g^{-1}) from offline calculations using CESMmet, as described in the text. Also shown is the mean of $MR_{BC,snowfall}$ after weighting by the snowfall amount in snow water equivalent. The arithmetic mean and standard deviation of $[MR_{BC,snowfall}]_d$ are not given because it includes infinite mixing ratios (i.e. when snowfall is zero) and so these are not finite values.

		$[MR_{BC,snowfall}]_d$ & $[MR_{BC}]_d$	$[MR_{BC,snowfall}]_m$ & $[MR_{BC}]_m$	$[MR_{BC,snowfall}]_y$ & $[MR_{BC}]_y$
Greenland				
$[MR_{BC,snowfall}]_{d,m,y}$	median	48.1	7.4	5.2
	snowfall-weighted mean	7.2	8.3	8.3
$[MR_{BC}]_{d,m,y}$	mean	11.5	6.5	4.5
	median	8.4	6.2	4.3
	std dev.	7.8	4.3	1.9
North America				
$[MR_{BC,snowfall}]_{d,m,y}$	median	156.5	19.3	15.7
	snowfall-weighted mean	22.5	31.0	31.1
$[MR_{BC}]_{d,m,y}$	mean	12.4	7.3	6.1
	median	8.3	5.6	4.8
	std dev.	11.9	5.5	4.4
Eurasia				
$[MR_{BC,snowfall}]_{d,m,y}$	median	116.3	29.1	21.7
	snowfall-weighted mean	38.3	48.8	48.9
$[MR_{BC}]_{d,m,y}$	mean	27.9	20.0	22.4
	median	17.4	14.4	16.6
	std dev.	22.4	12.4	12.8

Table 4. Medians of the ratios, $[MR_{BC}]_d$: $[MR_{BC}]_y$, shown in Figures 4-5 and S1-S3 for our three study regions, using CESMmet and CRUNCEPmet. Means and standard deviations are not given because infinite mixing ratios in a few model grid boxes yield non-meaningful values.

Greenland				North America			Eurasia		
DJF	MAM	JJA	Annual	DJF	MAM	Annual	DJF	MAM	Annual
CESMmet									
2.24	2.51	2.33	2.34	1.64	1.58	1.57	1.60	1.54	1.53
CRUNCEPmet									
2.14	1.97	2.36	2.17	1.53	1.46	1.47	1.66	1.37	1.46

Figure 1. Examples of wet (left axis) and dry (right axis) BC mass deposition fluxes in CAM4 for year 2000 for a) two model gridboxes in Greenland containing the Dye-2 (69.2°N, 315.0°E) and Summit research stations (72.3°N, 321.7°E), and b) a single model gridbox in northern Eurasia (71.1°N, 85.0°E).

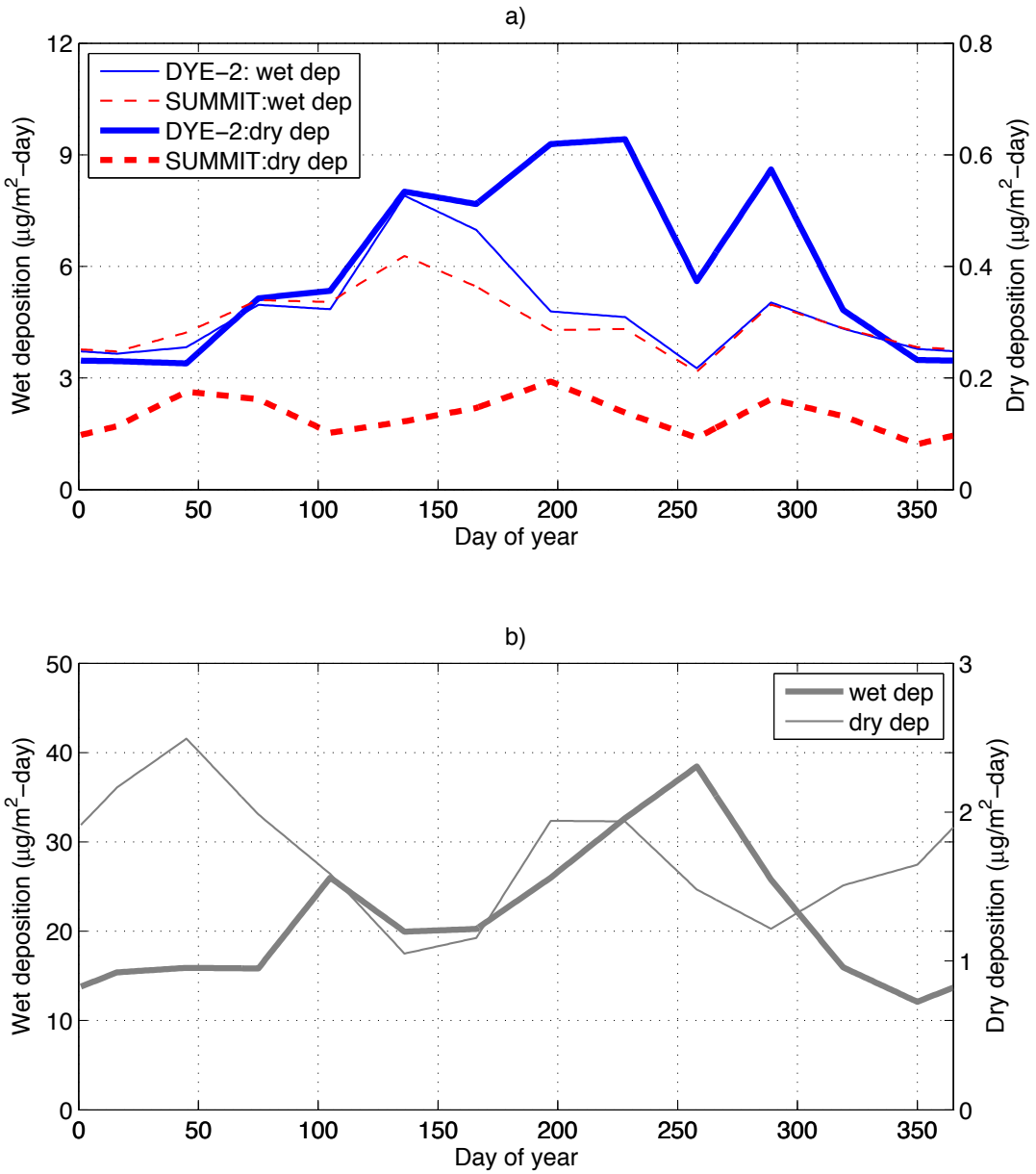

Figure 2. Relative frequency distributions of daily mixing ratios of BC in snowfall calculated using three different pairings of BC mass deposition fluxes and snowfall rates, as described in the text: a.) $[MR_{BC,snowfall}]_d$, b.) $[MR_{BC,snowfall}]_m$ and c.) $[MR_{BC,snowfall}]_y$. Note the differences in scale in a) versus in b) and c). Data shown are for model snowfall rates for year 2000 (CESMmet runs) and for the Dye-2 Greenland gridbox as shown in Figure 1a.

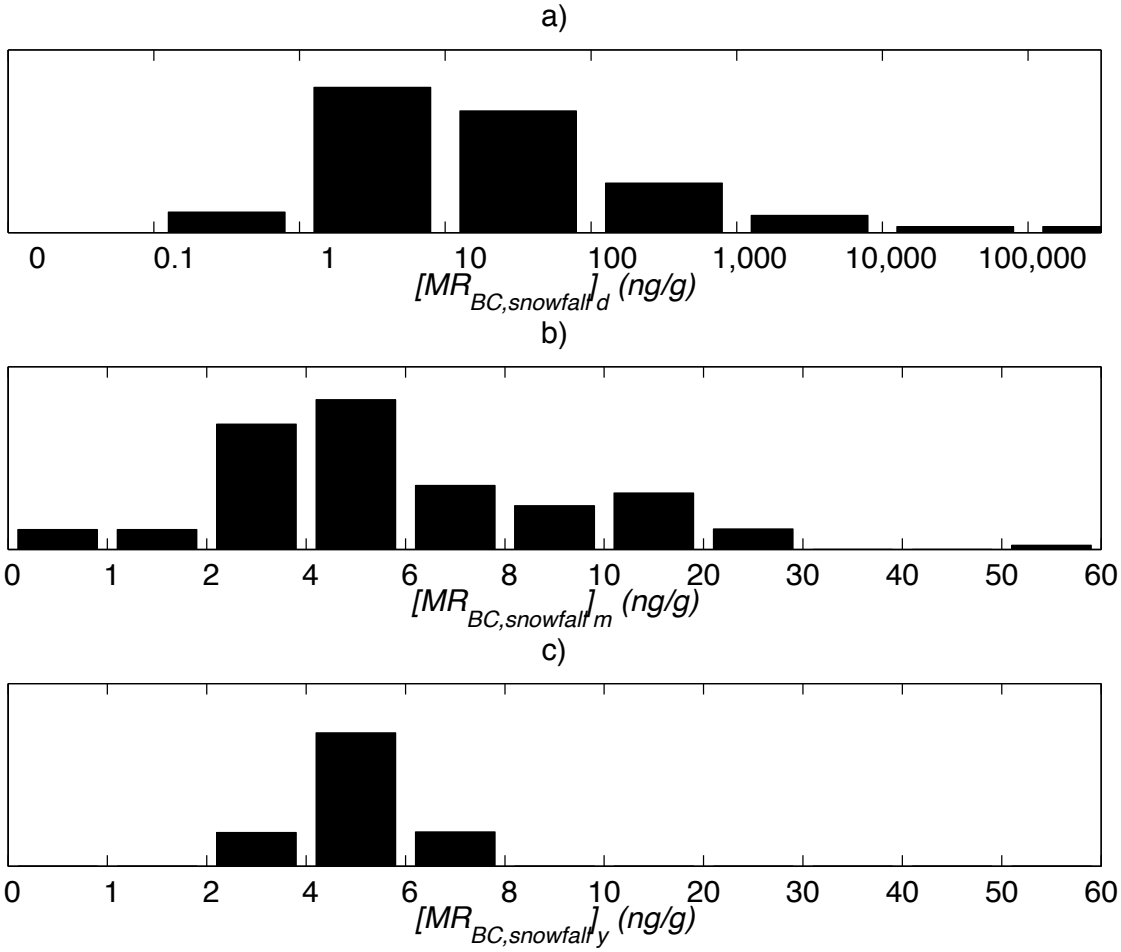

765 **Figure 3.** Surface snow BC mixing ratios (MR_{BC}) for a) the Dye-2 gridbox shown in
766 Figure 1a and Figure 2 and b) the same northern Eurasia gridbox shown in Figure
767 1b. Shown are the average (red diamonds) and standard deviation (red shaded
768 area) across ten years of $[MR_{BC}]_d$ from the offline computation using CESMmet and
769 10-year averages of MR_{BC} values from CESM-CAM4 runs using prescribed aerosol
770 deposition fields, $[MR_{BC}]_{model,prescr}$ (black dots). The CESM-CAM4 values (black dots)
771 include the effects of snow water loss to sublimation and melting, whereas the
772 offline calculations (red) do not. Also shown are $[MR_{BC}]_m$ (blue circles) and $[MR_{BC}]_y$
773 (green x's) from the offline calculation, again using CESMmet.
774

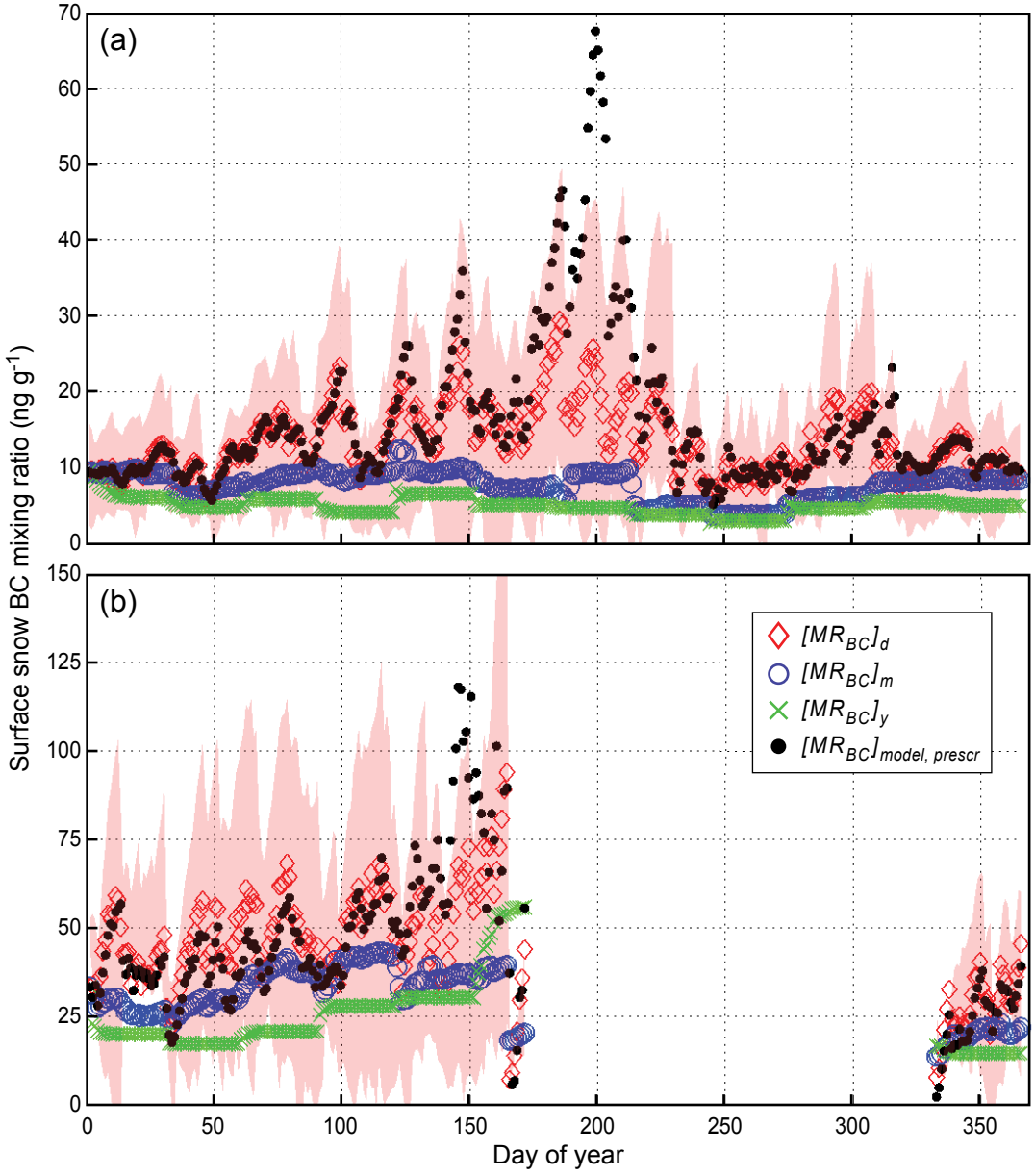

775

Figure 4. Histograms of the ratios $[MR_{BC}]_d$:$[MR_{BC}]_y$ for all gridboxes in the regions around a) Greenland, b) Eurasia and c) North America. Shown are seasonal averages for winter (DJF), spring (MAM) and summer (JJA; Greenland only) of daily values when the offline calculations use CESMmet. Ratios $[MR_{BC}]_d$:$[MR_{BC}]_y$ > 5.0 are allocated to the 5.0 bin. (See Figures S1-S3 for maps of the seasonal averages of $[MR_{BC}]_d$:$[MR_{BC}]_y$ in each model gridbox in these three regions).

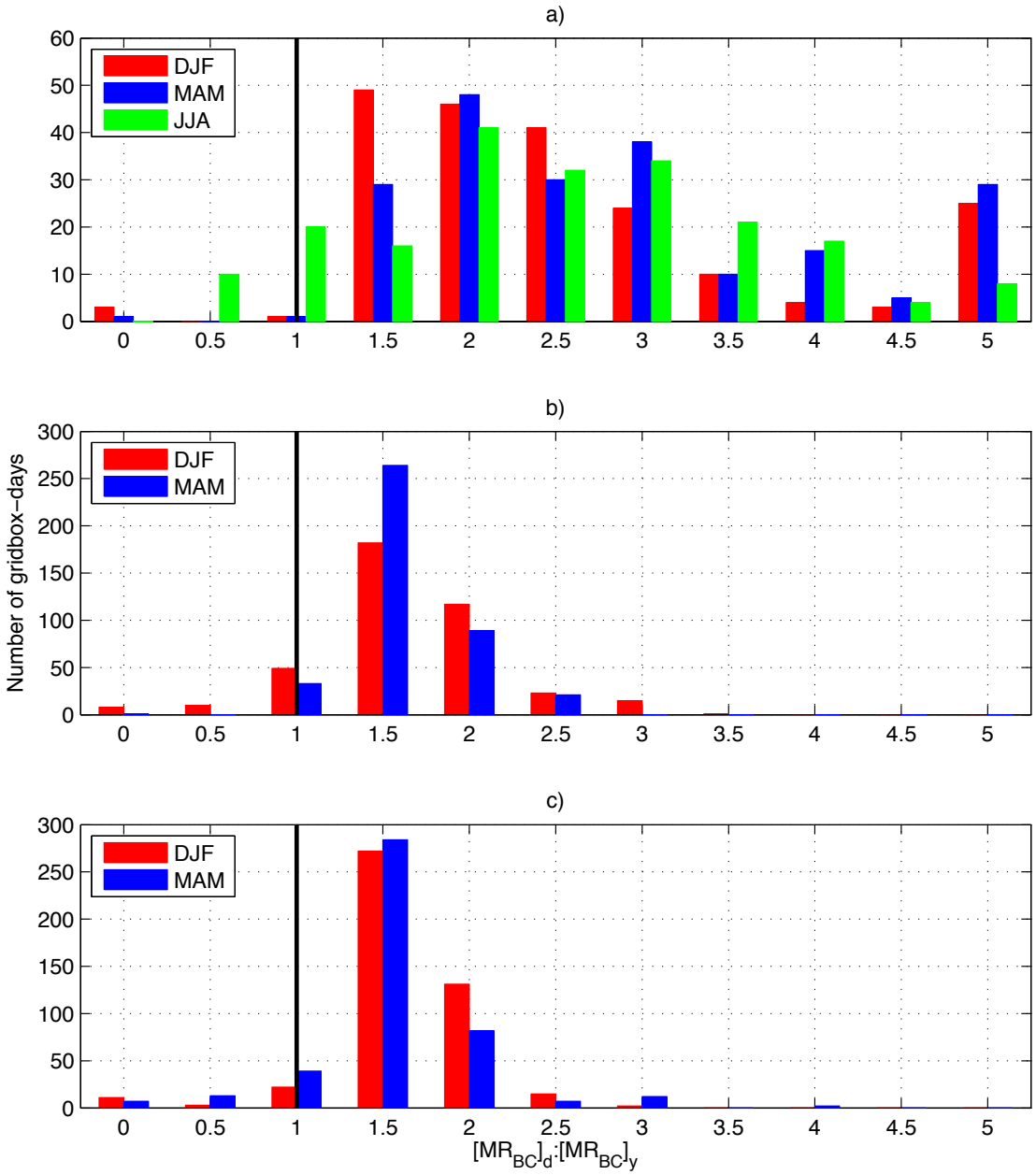

Figure 5. As in Figure 4, but for offline calculations using the CRU/NCEP reanalysis $SWE_{snowfall}$ data to calculate $MR_{BC,snowfall}$ and therefore $[MR_{BC}]_d$:$[MR_{BC}]_y$.